International Journal of Chemical and Biochemical Sciences
(ISSN 2226-9614)

Journal Home page: www.iscientific.org/Journal.html

Formulation and characterization of *Commicarpus chinensis* nanophytosomes for improved solubility and in vivo bioavailability

Kasireddy Paul Babu*[1], P. Shanmugasundaram[2]

[1]*Technology and Advanced Studies (VISTAS), Pallavaram, Chennai, Tamil Nadu, India*

[2]*Technology and Advanced Studies (VISTAS), Pallavaram, Chennai, Tamil Nadu, India*

Abstract

The *Commicarpus chinensis* exhibits several pharmacological actives like antibacterial, anticancer, antioxidant, chemo-preventive and anti-inflammatory properties. However till date, no studies have been reported on their nanophytosomes efficacy, especially in treating hepatoprotective activity because of poor solubility and bioavailability. Hence in the present study, an attempt has been made to load the extract into a single nanoparticlulate system to enhance their bioavailability and efficacy. This novel nanophytosomes was prepared by film-dispersion technique and was evaluated for particle size and shape using Zeta Sizer, Scanning Electron Microscopy (SEM) and Fourier Transform Infra-red (FT-IR) Spectroscopy. The optimized formulation was further subjected to in vitro and in vivo evaluations. The prepared nanoparticles were in the size range of 100 nm. In-vivo pharmacokinetic studies were carried in rats and the pharmacokinetic profile was studied. The comparative bioavailability results, of standard drug exhibited distinct characteristics, with AECC nanophytosomes offers advantages in terms of higher concentration of the drug, prolonged half-life, and potentially improved therapeutic efficacy compared to the standard drug.

Keywords: Alcoholic, Drug, Extract, Infrared, Phytosomes, Pharmacokinetic.

Full length article **Corresponding Author*, e-mail: pharmarxpro@gmail.com

1. Introduction

Commicarpus chinensis (CC), belonging to the Nyctaginaceae family, is commonly known as diffuse hogweed and is characterized as a perennial herb. Primarily thriving in warmer climates, this medicinal plant is widely distributed across tropical regions, encompassing India, China, and Pakistan [1]. Despite its historical use in traditional Indian medicine for ailments such as hepatitis, gonorrhea, antiulcer, and diabetes, the actual efficacy of *Commicarpus chinensis* remains uncertain [2]. A wealth of literature exists, detailing the potential therapeutic benefits of *Commicarpus chinensis*. However, its clinical application faces challenges due to inherent limitations, notably poor solubility and low bioavailability. In a study involving oral administration of a *Commicarpus chinensis* extract (500 mg/kg) to rats, a mere 52% bioavailability was observed, highlighting a significant hurdle in harnessing its medicinal properties effectively. To overcome these limitations, there is a pressing need for innovative formulation strategies to enhance the delivery of *Commicarpus chinensis.* Improving its solubility and bioavailability could unlock the full therapeutic potential of this herb, making it more viable for various medical applications [3,4]. Researchers and pharmaceutical developers may explore novel techniques and technologies to address these challenges, such as nanoformulations, lipid-based carriers, or other advanced drug delivery systems [5]. By doing so, *Commicarpus chinensis* could become a more promising herbal drug for future pharmaceutical and medicinal developments.

2. Materials and methods

2.1 Chemicals

Poloxamer 188 obtained from Sigma-Aldrich, Bangalore, India. PEG 6000, PEG 4000, PEG 1500 and Glutaraldehyde obtained from Niram chemicals, Mumbai, India. Silymarin was purchased from Micro Labs, Tamilnadu, India. Rat's feed was once supplied from mahaveer endeavors, madipally and hyderabad, India. Other chemicals and reagents for this investigation had been of diagnostic grade**.**

2.2 Preparation of extract loaded mixed micelles

The film-dispersion technique was used to prepare *Commicarpus chinensis* crude extracts loaded mixed micelles (MMs). The co-polymeric compositions (Table 1) were dissolved in 10ml of methanol for 5 minutes using a bath ultrasonication. The solvent (methanol) was vaporized at room temp, and the film generated at the bottom of the beaker

was dispersed using 10ml of de-ionized (doubled-distilled) water for 5 minutes using a bath ultrasonication. The obtained mixed micellar preparations were visually evaluated for complete extract solubilization, and observations were reported [6].

2.3 Characterization of nanoparticles [7]

2.3.1 Particle size and surface morphology

The particle size and surface characteristics were determined using SEM. After the nanoparticle formulations F1 to F3 had fully dried, images of the samples were taken.

2.3.2 Drug entrapment efficiency

The success of entrapping nanoparticles can be assessed using both direct and indirect methods. In the indirect method, centrifugation was used to determine the free quantity in the supernatant. The entrapment effectiveness was calculated as the difference between the initial drug quantity and the free or unentrapped quantity of drug in the supernatant with regard to the total quantity included in the nanocarrier preparation [8]. In the direct method, on the other hand, nanocarriers were dissolved in a suitable solvent and analyses after filtering and a reasonable dilution to determine the level of entrapment. The medication content percentage was used to calculate the incorporation efficiency.

Entrapment efficiency %= (Weight of the drug in nanoparticles)/ (Weight of the nanoparticles) X100

2.3.3 Zeta potential (ZP)

ZP can be used to measure the electric charge of nanoparticles at to evaluate the stability of particles. Using a Zetasizer Nano ZS (Malvern Instruments) formulations zeta potential was measured [9].

2.3.4 Solubility studies

The solubility of nanoparticles was determined using the USP rotating paddle apparatus at 100 rpm at 37 ± 0.5 ºC [10]. To the 500 ml of the dissolution medium, 100 mg of the formulation was added and mixed thoroughly. At intervals of "30 minutes, 1, 2, 4, 6, 8, 12, and 24 hours", aliquots of five ml were taken using a syringe filter (0.2 sterile filter), and the new medium was introduced. The samples were measured using a 425 nm UV-Vis spectrophotometer for analysis.

2.3.5 Drug Excipient Compatibility Studies [11]

Utilizing a Fourier transform infrared spectrophotometer, the spectra of AECC, Poloxamer-188, PEG 6000, PEG 4000, PEG 1500, and nanoparticle formulations F1, F2, and F3 were all obtained. 5 mg of the sample and dry KBr IR powder are mixed to get fine powder. This was squeezed under pressure for around 3 minutes over the wave number range 400-4000 cm-1 to capture the unique peaks of numerous samples. A thermal analytical method called differential scanning colorimetry (DSC) can be used to investigate how a test sample changes physically from one form to another. 10 mg of AECC, F1, F2, and F3 samples were heated between 0 °C and 400 °C at a rate of 10 °C/min in an open aluminium pan for analysis. Magnesium was chosen as the gold standard. The subsequent temperature variations were recorded.

2.3.6 Animal model and grouping

An experimental study was carried out on Wister albino rats of either sex (M/F) rat's age two months. Their body weights ranged from 150 to 200 g. Animals were maintained under standard laboratory aseptic conditions (12-h light/dark cycle, 24hrs). The food in the form of dry pellets and water is provided *ad libitum*. All the animals were approved by the ethics approval committee of the institute (Reg. No. 1636/PO/Re/S/12/ CPCSEA).

2.4. Pharmacokinetic Study of Phytosomes

Pharmacokinetic of drugs following their administration from dosage forms is an integral part of part of research investigations in order to obtain vital information with respect to bioavailability of the newly developed dosage forms [12].

2.5. Study Design

In the present research parallel study was utilized for determination of bioavailability parameters or pharmacokinetic parameters. Twenty Four Wistar rats were randomly split into four groups, for each group comprising 6 animals.

Group I: Control (Only CMC and free access to water)
Group II: Disease Control
Group III: AECC phytosomes
Group IV: Standard drug (Silymarin)

2.5.1. Preparation of sample solutions

All rats were fasted overnight, the nanophtosomes were administered by oral route. Rats were placed in metabolic cages and blood samples were collected by using 27-gauge needles from the caudal vein into heparinized tubes at time intervals of 0, 1, 2, 4, 6, 8,10,12,14 and 24 hours. Xylene was applied to the shaved caudal vein, which causes blood vessel to dilate. The samples were subjected to centrifugation by adding 100µl of Acetonitrile cyclo mix at 8000 rpm for 30 mins and the supernatant was collected by using micropipette. After filtration 20 µl sample was injected into the HPLC system.

2.5.1.1. Chromatographic parameters

- Equipment: High performance liquid chromatography equipped with Auto Sampler and PDA detector (Waters-module 2695)
- Column: Spursil ODS C18 (4.6 x 150mm, 5 □m)
- Mobile Phase: 55:45(ACN:0.2% OPA)
- Flow rate: 1.0 ml/min
- Injection volume: 20 µl
- Temperature: Ambient
- Run time: 10.0 min
- Centrifuge: Hermle microliter centrifuge Z100 (model no 292 P01)
- Cyclomixer: Remi equipment (model no- CM101DX).

2.5.1.2. Preparation of standard Stock solution of Phytosomes (100µg/ml)

Accurately weighted 100 mg phytosomes were transferred into a 100 ml volumetric flask to this add 70ml of diluent was added and sonicated to dissolve the powder drug completely and finally volume was made up to the mark with the same solvent (stock solution). Further 10.0 ml of the above stock solution was pipetted into a 100ml volumetric

flask and diluted up to the mark with diluent. Finally, the preparation was filtered through 0.22µm injection filter.

2.5.1.3. Preparation of 0.2 % OPA

0.2 ml pf orthophosphoric acid acid was taken in 100ml volumetric flask, dissolved and diluted to 100ml with HPLC water.

2.5.1.4. Preparation of mobile phase

Mobile phase was prepared by mixing 450 ml (45%) buffer and 550ml (55%) of Acetonitrile. The mixer was degassed in ultrasonic water bath for 5 minutes and filtered through 0.45 µ filter under vacuum.

2.5.1.5. Preparation of diluent:

Mobile phase was used as diluent.

2.5.1.6. HPLC method Validation in Plasma

20µl of drug free blank plasma and Phytosomes Solutions were injected to determine specificity. The linearity was estimated using in Specific range. The chromatograms were developed by injecting 20µl solution and the peak area was calculated for each drug solution and plotted the standard graphs and calculated correlation coefficient. To determine the inter and intraday precision repeated this study for six times. Method was validated for robustness, LOD, LOQ and accuracy.

2.5.1.7. Analysis of Pharmacokinetic Parameters

Non compartmental method was used for the estimation of pharmacokinetic parameters of Pure Extracts and Prepared Phytosomes and the concentration vs. time data.PK parameters were estimated by using Thermo Scientific KINETICA 5.2 software [13].

2.6. Statistical Analysis

With the help of Graph Pad Prism 6 software data was statistically analyzed. For comparison of PK parameters of test and control samples paired t-test was used and a value of $p<0.05$ was considered to be significant. ANOVA was used to determine any differences PK parameters obtained in a group (in six animals) [14].

3. Result and discussion

3.1. IR spectral studies

The spectra obtained from IR studies at wavelength range of 4000 cm^{-1}-400 cm^{-1} are shown in Fig. 1 to 4. The initial IR spectra of the selected of AECC (cm^{-1}): OH=3566.96; CH-Stretching=2972.40; C=O 1627.97; Aromatic CH=1429.30; C-O Stretching= 1280.78; Di substituted benzene= 1028.1. AECC + Poloxamer-188+ PEG 6000 Nanoparticles (cm^{-1}): NH = 3275.24; OH of COOH =2956.97; C-H Stretching =1122.61; C=O 1627.97; C-O Stretching =1375.29; C-N Stretching =1184.33; Aromatic CH =1234.48; Di substituted benzene =962.51. AECC + Poloxamer-188+ PEG 4000 Nanoparticles (cm^{-1}): NH 3419.90; OH of COOH 3019.58; C-H Stretching 2956.97; C=O 1695.54; C-O Stretching 1116.82; C-N Stretching 1153.47; Aromatic CH 1282.71; Di substituted benzene 977.94 FTIR data of AECC + Poloxamer-188+ PEG 1500 nanoparticles (cm^{-1}): NH 3419.90; OH of COOH 3049.56; C-H Stretching 2956.97; C=O; 1695.49; C-O Stretching 1122.61; C-N Stretching 1184.33; Aromatic CH 1234.48; Di substituted benzene 977.94. After interpretation of the above spectra it was confirmed that there was no shifting, loss or appearance of functional peaks between the spectra of AECC and mixture. From the spectra it was concluded that the drug was entrapped into the polymer matrix without any chemical interaction. From the IR study it was observed that, the selected polymer was found to be compatible for entrapping the selected drug as shown in Figure 1 to 4.

3.2. Pre formulation studies results

Poor solubility leads to poor dissolution, therefore to enhance the dissolution of the drug; different techniques have been employed such as particle size reduction by forming nanoparticles which is a novel technique. The results were summarized in table no. 2.

3.3. Characterization of AECC nanoparticles

3.3.1. Entrapment efficiency

In AECC nanophytosomes the percent drug encapsulated for F1formulation is 96.6, F2 is 96 and F3 is 95.8 respectively. Therefore the percent entrapment efficiency is almost similar in all the three formulations. The results were shown in table no.3.

3.3.2. Particle size of AECC formulations

The AECC nanoparticles show the particle size distribution in the range of 100-200 nm as measured by photon correlation spectroscopy using a Malvern Zetasizer Nano ZS 90 zeta potential technique as shown in Fig. 5. The Average Particle size (nm) of F1 198nm, F2 179nm and F3 112 nm. The result revealed that increase in the stirring time results in increase in particle size due to the formation of aggregates. Similarly decrease in the stirring time results in increase in particle size due to increase in ionic strength of the compounds. It is also evident that the formed nanoparticle was monodispersed. The external surface morphology study of the prepared nanoparticles was carried out by using SEM. The particle size was observed to be in the range of 100 nm. The SEM images show that the prepared nanoparticles have a spherical and rectangular morphology shows. The surface morphology and the particle size of the nanoparticles were uniform shown in figure 5. The figure-6 shows that AECC formulations Zeta potential Data wasF1-33±5, F2-31±7and F3-32±3.

3.3.3. XPRD analysis

We may infer from XRPD graphs that the drug's crystallanity altered in the NS (Figure 7). When compared to the peaks of AECC, the peaks produced for the pure drug were extremely clear and crisp, and their intensity was also quite high. The peak intensity decrease is a sign that the drug's tendency to crystallise has diminished.

3.4. Pharmacokinetic Results

In the present research parallel study was utilized for determination of bioavailability parameters or pharmacokinetic parameters. Twenty-four Wistar rats were randomly split into four groups, for each group comprising 6 animals was used pharmacokinetics studies.

Table 1: Formulation and optimization of Alcoholic extract of *Commicarp us chinensis* (AECC)

Formulation	F-1	F-2	F-3
AECC	100	100	100
Poloxamer-188 (mg)	100	250	500
PEG (6000) (mg)	20	-	-
PEG (4000) (mg)	-	20	-
PEG (1500) (mg)	-	-	20
Ethanol (mL)	8	8	8
Distilled H_20 (mL)	2	2	2
Glutaraldehyde (8% V/V) (mL)	0.11	0.11	0.11
Observation after dilution with water up to 10mL	X	X	(Soluble)

Table 2: Preformulation studies for drug AECC

Physicochemical properties	Results
Appearance	Yellow in color
Shape	Crystalline in shape
Solubility	Water insoluble
Melting point	183^{o}C

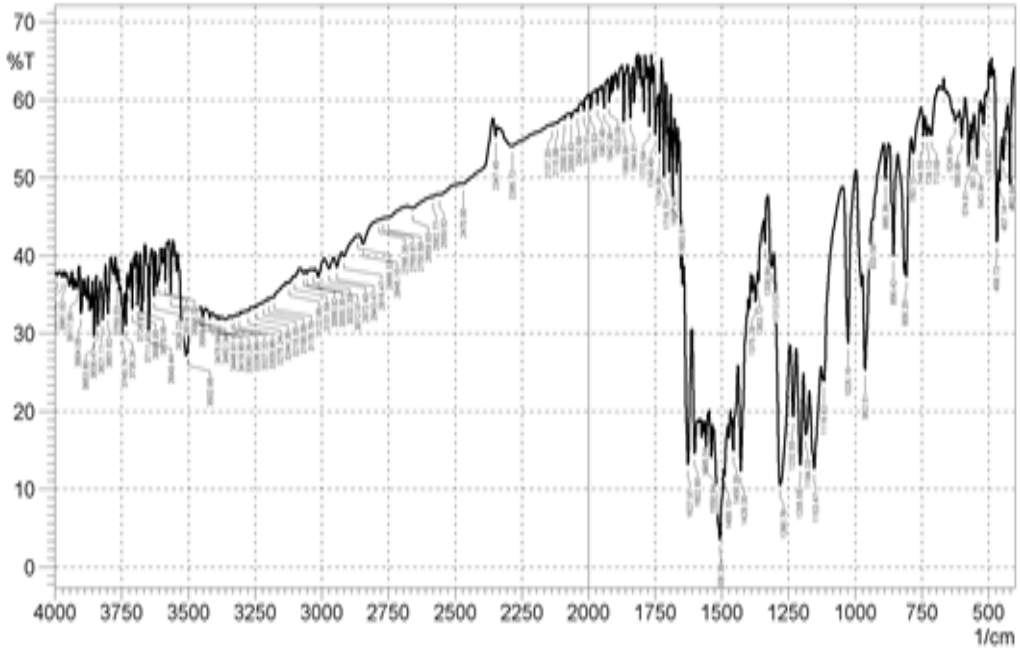

Figure 1: FT-IR graph of AECC

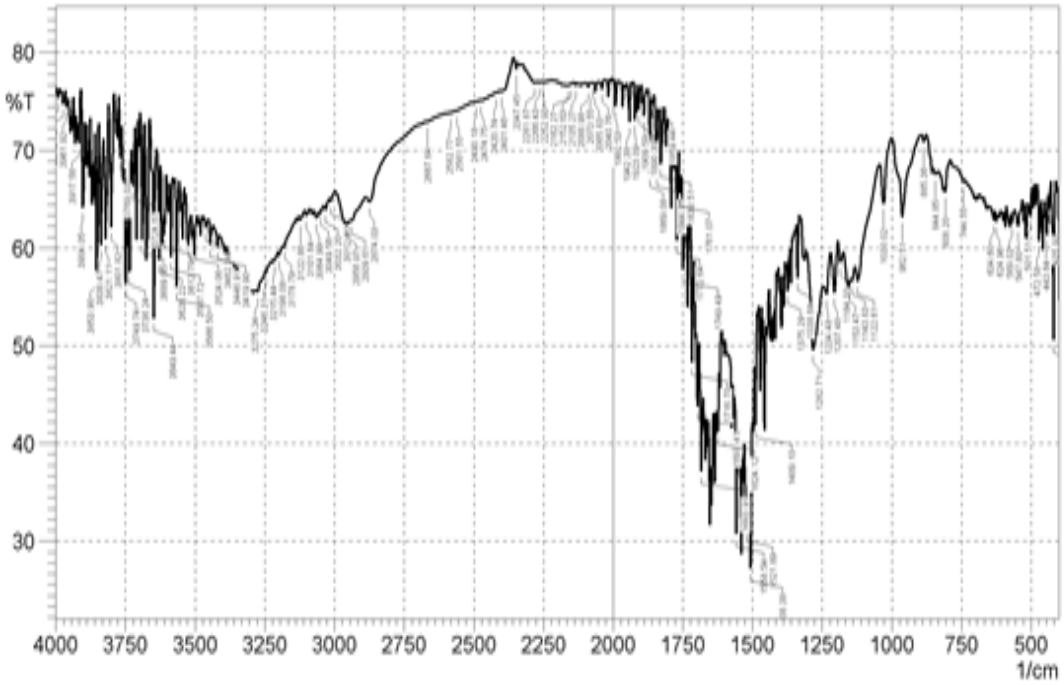

Figure 2: FT-IR graph of AECC + Poloxamer-188+ PEG 6000 Nanoparticles

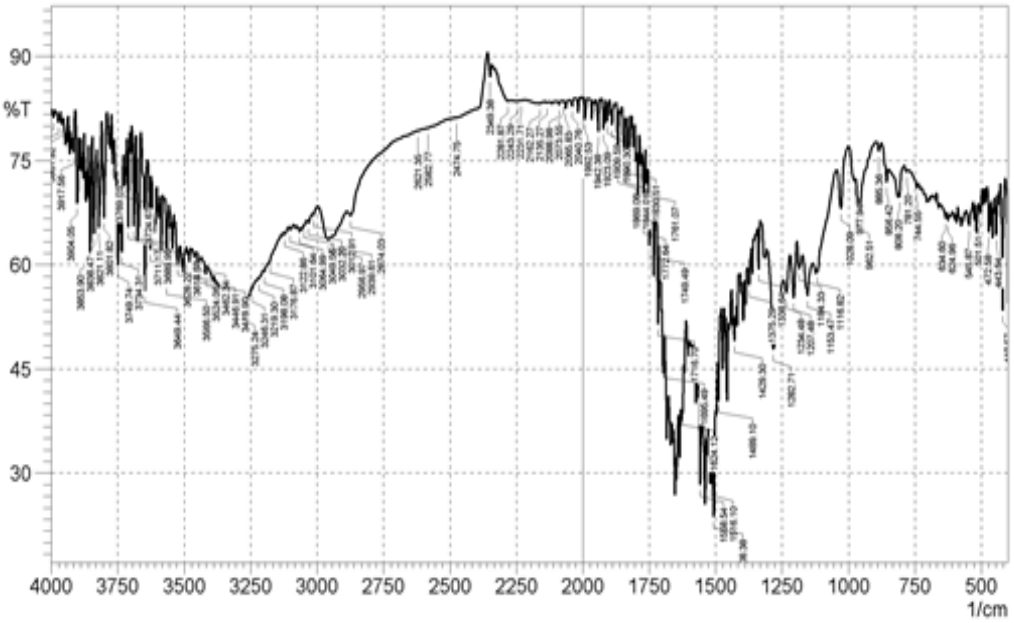

Figure 3: FT-IR graph of AECC + Poloxamer-188+ PEG 4000 Nanoparticles

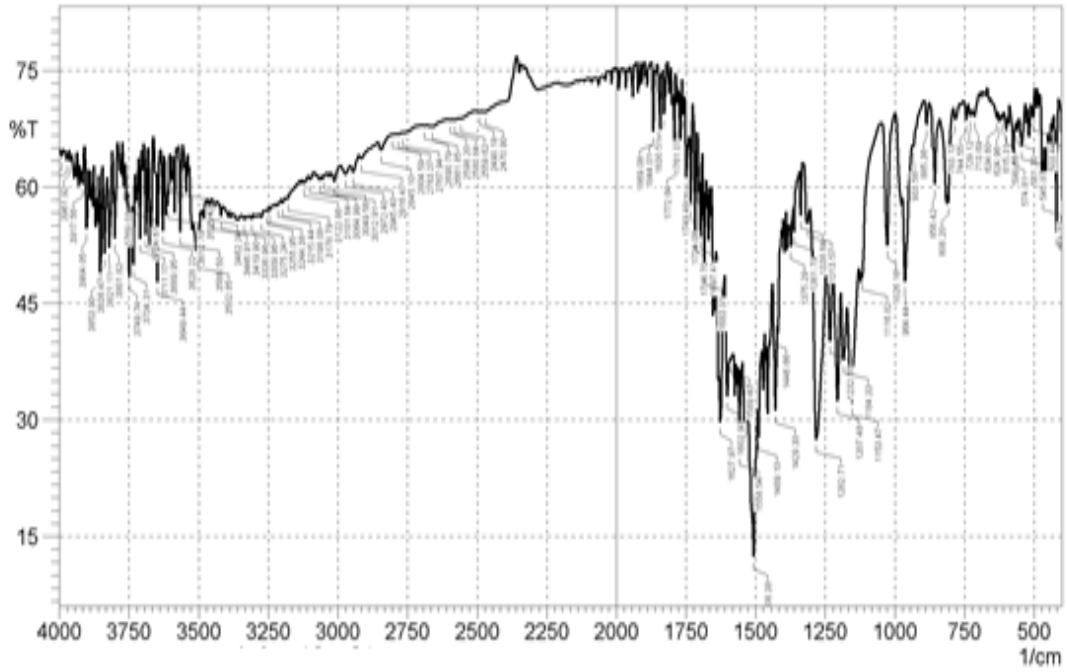

Figure 4: FT-IR graph of AECC + Poloxamer-188+ PEG 1500 nanoparticles

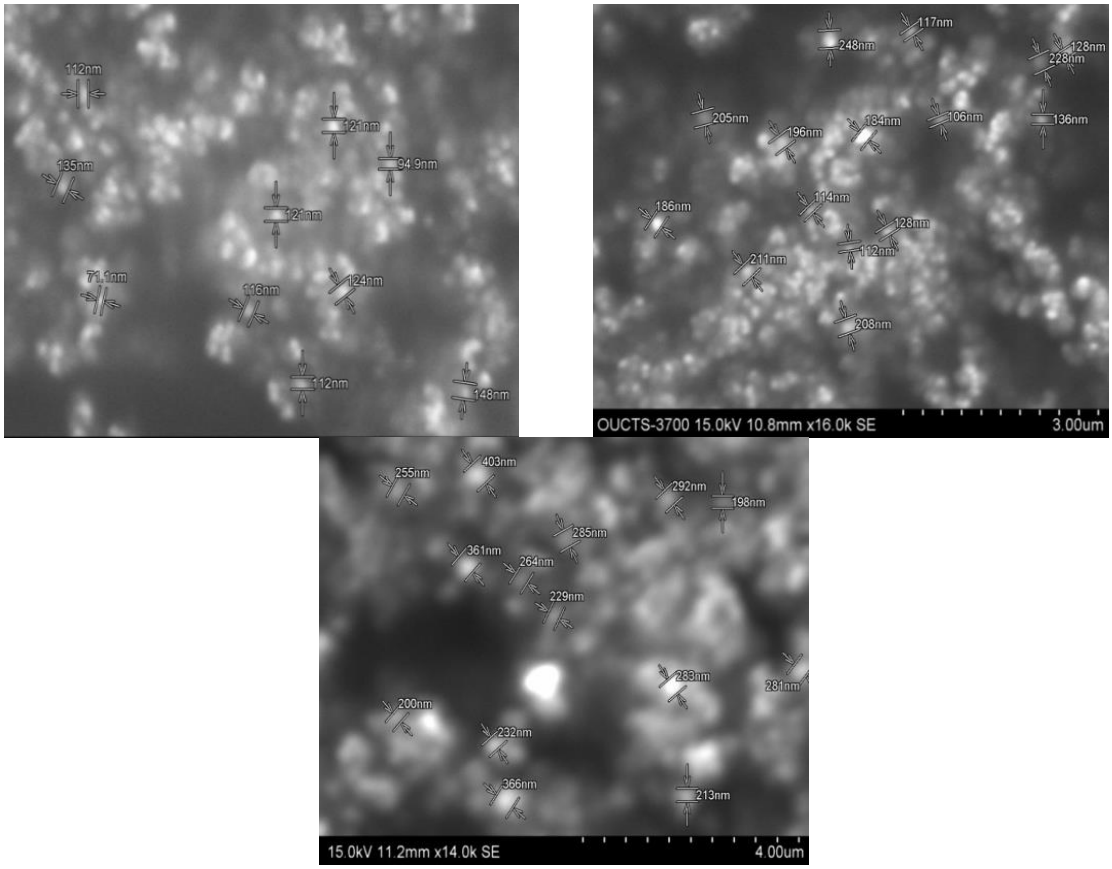

Figure 5: SEM pictures of AECC nanoparticles (F1, F2 and F3)

Table 3: Percent Entrapment efficiency of AECC nanoparticle formulations

Formulations	% Drug Encapsulated
F1	96.6±2.5
F2	96±2.3
F3	95.8±3.5

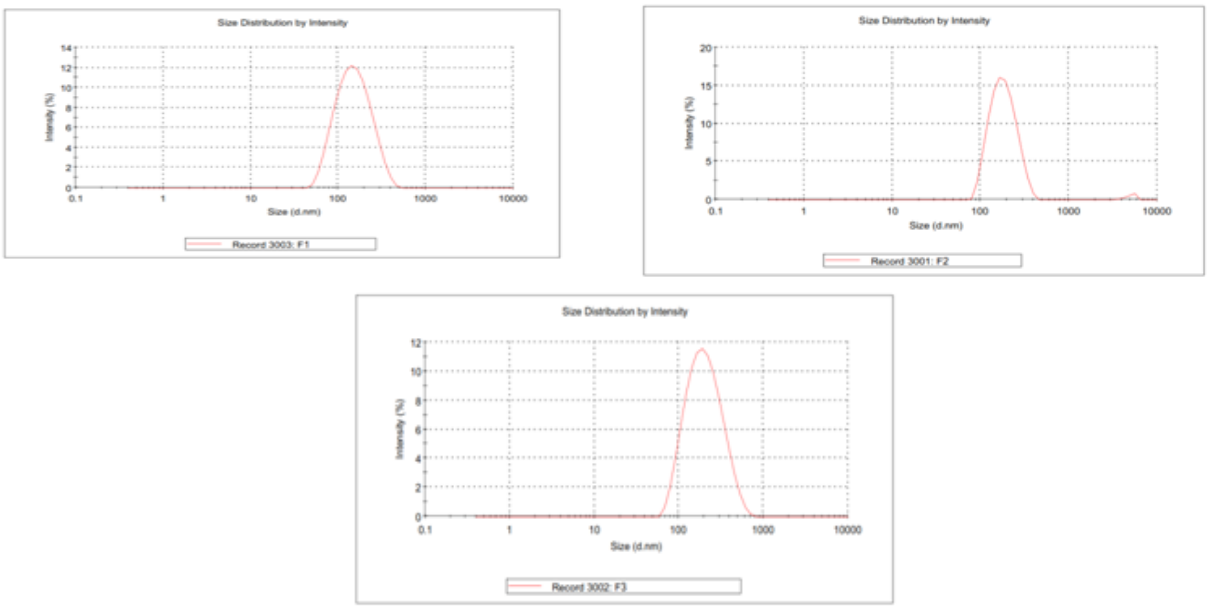

Figure 6: Zeta potential Data of AECC nanoparticles (F1, F2 and F3)

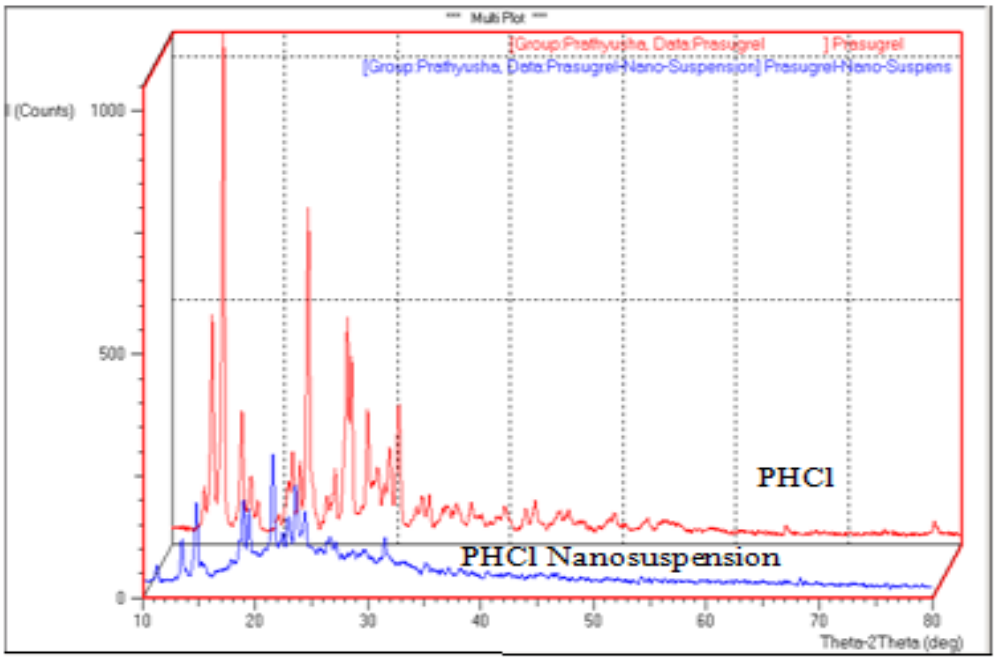

Figure 7: XRD graph of AECC

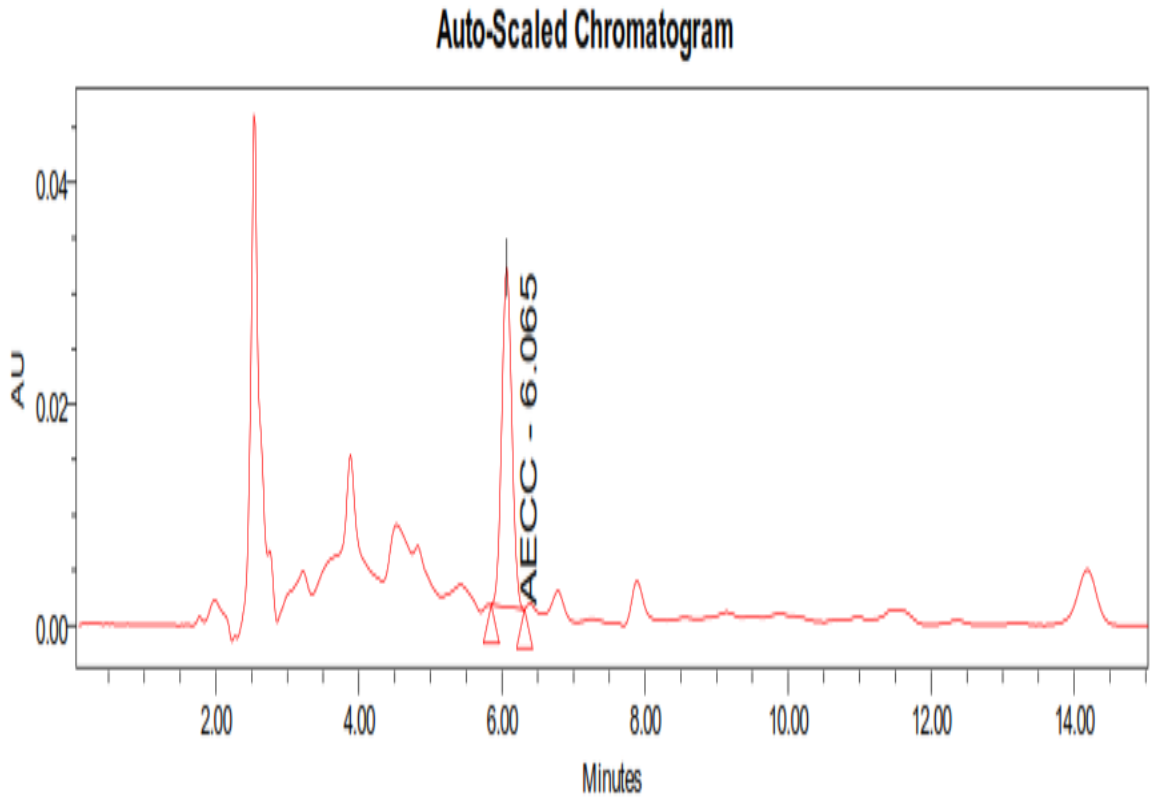

Figure 8: Chromatogram of AEC

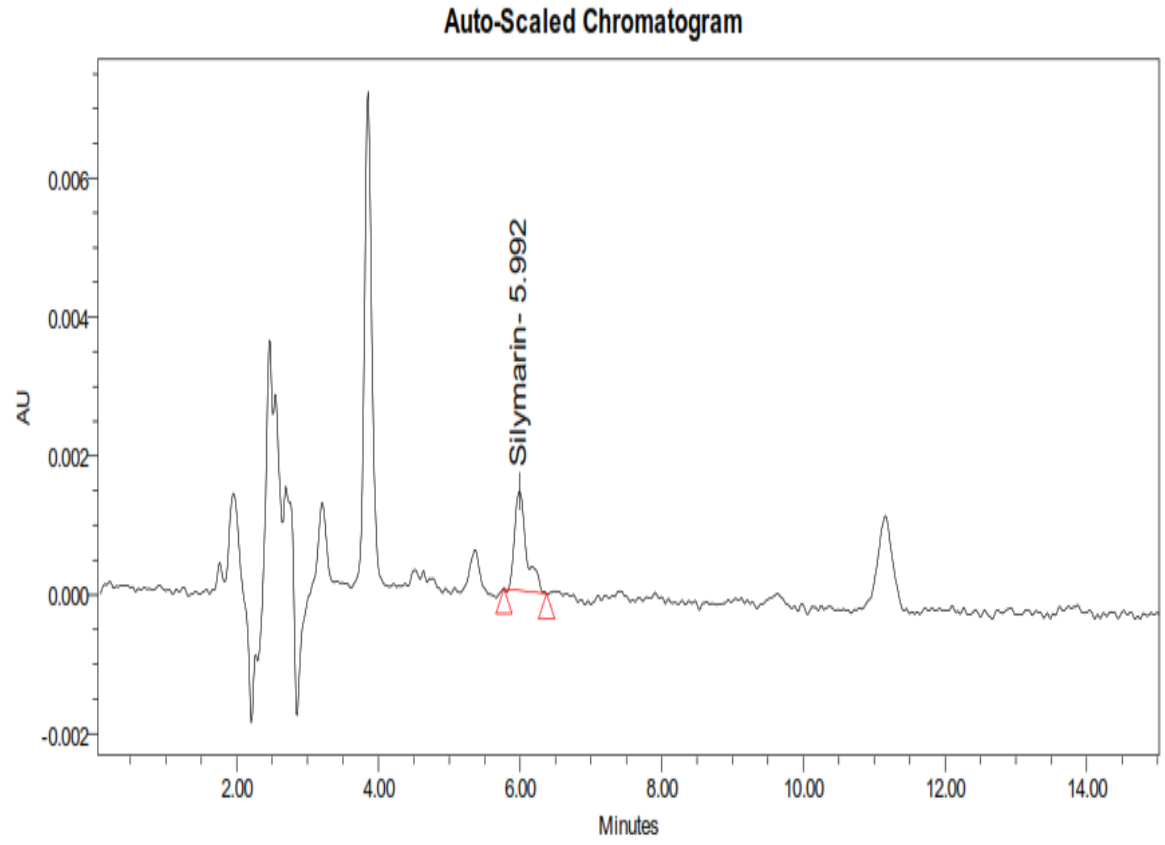

Figure 9: Chromatogram of Standard drug

Table 4: Pharmacokinetics studies of AECC Phytosomes and Standard

PK parameter	AECC phytosomes	STD Drug (Silymarin)	't' test at 0.05
C_{max} (µg/mL)	452.66	398.12	significant
T_{max} (Hours)	1.20	1.14	Significant
$t_{1/2}$ (hrs)	2.05	1.85	Significant
MRT (h)	0.076	0.085	Significant
Total AUC (µg-hr/mL)	156.85	142.22	Significant
Total AUMC (µg-hr/mL)	855.36	653.25	Significant
Cl (mL/min)	1.33	1.25	Significant
K_{el} (hrs^{-1})	0.022	0.12	Significant

The mean plasma concentration versus time profiles and pharmacokinetic parameters are shown in Figure 8 and Table 4. Pharmacokinetic parameters such as peak plasma concentration (C_{max}), time to peak concentration (tmax), area under the plasma concentration-time curve (AUC_{0-t}), $AUC_{0-\infty}$), elimination rate constant (kel) and elimination half-life (t1/2) were calculated separately and the blood level data of selected formulations were compared and are presented in Table 4 and the results were calculated using the trapezoidal method. The data revealed that among the developed nanophytosomes have higher bioavailability when compared with standard drug. The increase in the bioavailability may be due to reduce in the particle size leads in the nanonisation, absorption in the gastrointestinal (GI) tract and increased permeability of the drug by surfactants by increase surface area. This increase may be due to the prepared nanoparticle are embedded into the phospholipid bilayer which reduces the bacteria exposure and enzymatic degradation during the process of absorption which ultimately allows the drugs to extent contact with the intestinal wall and shows adhesive property toward the small intestine and epithelial mucosal surface.

4. Conclusion

The IR spectra it was concluded that the drug was entrapped into the polymer matrix without any chemical interaction and it was observed that, the selected polymer was found to be compatible for entrapping the selected drug. In SEM analysis the particle size was observed to be in the range of 100 nm and SEM images shows that the surface morphology and particle size of the nanoparticles were uniform. AECC phytosomes demonstrates a higher Cmax and Total AUMC compared to standard drug silymarin, indicating potentially improved bioavailability and increased exposure to the drug. The longer half-life of AECC phytosomes suggests a prolonged duration of drug action, which could be beneficial for maintaining therapeutic levels. The longer Tmax for AECC phytosomes indicate a slower rate of absorption, but the higher Cmax compensates for this, potentially leading to sustained drug release. In summary, based on the comparative bioavailability results, of standard drug exhibited distinct characteristics, with AECC nanophytosomes offers advantages in terms of higher concentration of the drug, prolonged half-life, and potentially improved therapeutic efficacy compared to the standard drug.

Conflict of interest

None

References

[1] D K Ved, Suma Tagadur Sureshchandra, Vijay Barve, Vijay Srinivas, Sathya Sangeetha, K. Ravikumar, Kartikeyan R., Vaibhav Kulkarni, Ajith S. Kumar, S.N. Venugopal, B. S. Somashekhar, M.V. Sumanth, Noorunissa Begum, Sugandhi Rani, Surekha K.V., and Nikhil Desale. (2016). (envis.frlht.org / frlhtenvis.nic.in). FRLHT's ENVIS Centre on Medicinal Plants, Bengaluru.

[2] B. Manas, Y. Rajesh, V.R. Kumar, B. Praveen, K. Mangamma. (2010). Extraction, phytochemical screening and in-vitro evaluation of anti-oxidant properties of Commicarpus chinesis (aqueous leaf extract). International Journal of pharma and bio sciences. 1(4).

[3] T. Pullaiah. (2006). Encyclopedia of world medicinal plants. Vol.1:337.

[4] D. Vanila, S. Ghanthikumar, V. Manickam. (2008). Ethanomedicinal uses of plant Commicarpus chinensis. Ethnobotanical Leaflets. 12(15): 1198-205.

[5] B.V. Bonifacio, P.B. da Silva, M.A.d.S. Ramos, K.M.S. Negri, T.M. Bauab, M. Chorilli. (2014). Nanotechnology-based drug delivery systems and herbal medicines: a review. International journal of nanomedicine. 1-15.

[6] S. Feng, Z. Zhang, A. Almotairy, M.A. Repka. (2023). Development and evaluation of polymeric mixed micelles prepared using Hot-melt extrusion for extended delivery of poorly water-soluble drugs. Journal of Pharmaceutical Sciences.

[7] N. Joudeh, D. Linke. (2022). Nanoparticle classification, physicochemical properties, characterization, and applications: a comprehensive review for biologists. Journal of Nanobiotechnology. 20(1): 262.

[8] V. Maravajhala, N. Dasari, A. Sepuri, S. Joginapalli. (2009). Design and evaluation of niacin microspheres. Indian Journal of Pharmaceutical Sciences. 71(6): 663.

[9] J.A. Barbosa, M.S. Abdelsadig, B.R. Conway, H.A. Merchant. (2019). Using zeta potential to study the ionisation behaviour of polymers employed in modified-release dosage forms and estimating their pKa. International journal of pharmaceutics: X. 1: 100024.

[10] R. Abdelmonem, M.K. Younis, D.H. Hassan, M.A.E.-G. El-Sayed Ahmed, E. Hassanein, K. El-Batouty, A. Elfaham. (2019). Formulation and characterization of chlorhexidine HCl nanoemulsion as a promising antibacterial root canal irrigant: in-vitro and ex-vivo studies. International journal of nanomedicine. 4697-4708.

[11] S. Jain, R.P. Shah. (2023). Drug-Excipient Compatibility Study Through a Novel Vial-in-Vial Experimental Setup: A Benchmark Study. AAPS pharmscitech. 24(5): 1-13.

[12] H. Mirzaei, A. Shakeri, B. Rashidi, A. Jalili, Z. Banikazemi, A. Sahebkar. (2017). Phytosomal curcumin: A review of pharmacokinetic, experimental and clinical studies. Biomedicine & Pharmacotherapy. 85: 102-112.

[13] T. Jaki, M.J. Wolfsegger. (2012). Non-compartmental estimation of pharmacokinetic parameters for flexible sampling designs. Statistics in Medicine. 31(11-12): 1059-1073.

[14] M. Jendryka, M. Palchaudhuri, D. Ursu, B. van der Veen, B. Liss, D. Kätzel, W. Nissen, A. Pekcec. (2019). Pharmacokinetic and pharmacodynamic actions of clozapine-N-oxide, clozapine, and compound 21 in DREADD-based chemogenetics in mice. Scientific reports. 9(1): 4522.